

Published in IET Systems Biology
 Received on 28th May 2007
 Revised on 18th July 2008
 doi: 10.1049/iet-syb.2007.0028



Deconstructing the core dynamics from a complex time-lagged regulatory biological circuit

O. Eriksson^{1,2,3} B. Brinne^{2,3} Y. Zhou⁴ J. Björkegren²
 J. Tegnér^{2,3}

¹Stockholm Bioinformatics Center, AlbaNova, Stockholm University, Stockholm SE-106 91, Sweden

²The Computational Medicine Group, Center for Molecular Medicine, Department of Medicine, Karolinska Institutet, Karolinska University Hospital, Solna, Stockholm SE-171 76, Sweden

³Division of Computational Biology, Department of Physics, Chemistry and Biology, The Institute of Technology, Linköping University, Linköping SE-581 83, Sweden

⁴Department of Mathematics, Stockholm University, Stockholm SE-106 91, Sweden
 E-mail: jesper.tegner@ki.se

Abstract: Complex regulatory dynamics is ubiquitous in molecular networks composed of genes and proteins. Recent progress in computational biology and its application to molecular data generate a growing number of complex networks. Yet, it has been difficult to understand the governing principles of these networks beyond graphical analysis or extensive numerical simulations. Here the authors exploit several simplifying biological circumstances which thereby enable to directly detect the underlying dynamical regularities driving periodic oscillations in a dynamical nonlinear computational model of a protein–protein network. System analysis is performed using the cell cycle, a mathematically well-described complex regulatory circuit driven by external signals. By introducing an explicit time delay and using a ‘tearing-and-zooming’ approach the authors reduce the system to a piecewise linear system with two variables that capture the dynamics of this complex network. A key step in the analysis is the identification of functional subsystems by identifying the relations between state-variables within the model. These functional subsystems are referred to as dynamical modules operating as sensitive switches in the original complex model. By using reduced mathematical representations of the subsystems the authors derive explicit conditions on how the cell cycle dynamics depends on system parameters, and can, for the first time, analyse and prove global conditions for system stability. The approach which includes utilising biological simplifying conditions, identification of dynamical modules and mathematical reduction of the model complexity may be applicable to other well-characterised biological regulatory circuits.

1 Introduction

Molecular networks, defined by protein–protein, protein-to-gene and metabolic interactions, determine both the intrinsic cellular dynamics and the cellular response to external signals. In recent years, there have been extensive studies on characterising relatively well-known biological networks. Available and expanding resources of chemical binding information can be represented as metabolic, transcription

factor and protein–protein networks. As a rule, these networks have been analysed by graph theoretical methods simply characterising properties of the network wiring diagram [1]. An important current topic is how to integrate several data types in order to collect interactions from different sources and directly construct a network graph [2, 3] using algorithms [4]. In addition to topologically large-scale networks, there is now an increasing number of publications on the analysis of small-scale mathematical

dynamical models of important biological regulatory circuits such as circadian rhythms [5], segmentation genes [6], signal transduction pathways [7, 8], genetic switches [9] and oscillators [10]. Thus, a growing number of biological networks of different size and dynamical complexity stress the importance of developing methods for dissecting the core dynamics driving the complex circuit behaviour [11].

These molecular networks based on experimental data are large complicated nonlinear dynamical systems. In contrast, tools from dynamical system theory such as bifurcation analysis are most efficient for small systems. Thus, the analysis of these systems has largely been limited to either partial insights into small systems or exhaustive computer simulations [7, 8, 12]. A logical step in the analysis of molecular networks beyond large-scale network topology or dynamics is therefore to ask whether there exist simplifying operational principles for a variety of complex networks [13, 14]. Recently, there have been several studies in this direction, including identifying conditions for robustness in a large kinetic model of the *Drosophila* segmentation system [6], using a Boolean modelling approach [15], formulating a global condition for the control robustness in circuits for morphogenic gradients [16], successful investigation on an analytical technique for detecting multistability for positive-feedback kinetic systems [17], division of the cell cycle into excitation and relaxation periods based on the Jacobian of kinetic differential equations [18] and analysis of biochemical networks based on a linear system approach [19]. An additional complicating feature of many biological control systems is that there are time delays in the reaction kinetics caused by, for example, the transcription–translation process [20–22] or the signal transduction cascade.

Here we develop a mathematical approach to uncover what we refer to as effective regularities in the network dynamics, utilising several simplifying features inherent in the biological regulatory circuit. Therefore we essentially use the biology to reduce the complexity of the original hard mathematical problem of dissecting the behaviour of a nonlinear dynamical system with a time delay. We illustrate our approach by dissecting the cell cycle, one of the most extensively studied and essential regulatory circuits of biology. The computational model pioneered and developed by Novak *et al.* (NT-model) [23] describing the cell cycle regulation of fission yeast incorporates and accounts for a large body of experimental data [24]. This biological circuit includes biological but difficult mathematical features such as effective time delay and nonlinear dynamical interactions. We develop a reduction scheme, first conceptualised in Eriksson *et al.* [25] where our analysis reveals a governing piecewise linear (PL) system [26, 27] driving the cell cycle. This enables us not only to derive explicit conditions for cell cycle oscillations and expressions for cell mass but also to uncover the underlying dynamical landscape of the cell cycle.

The structure of the article is as follows. First we summarise the original NT-model of the cell cycle and the basic dynamics between the genes and proteins. In Section 3 we reduce the NT-model by identifying dependencies between the variables thereby finding effective dynamical modules in the NT-model. Using a time-lagged steady-state approximation we simplify the description of the modules thus setting the stage for a detailed mathematical analysis. In Section 4 we perform a dynamical analysis in two steps. First we identify and classify the fixed points, and derive explicit expressions for cell mass. In the second step we use the vector fields for performing a global analytical stability analysis of the cell cycle. We conclude the article with a discussion where we address the putative value as well as current limitations of our approach for identifying the underlying dynamical regularities driving complex dynamics in biological regulatory circuits.

2 Cell cycle dynamics in the NT-model

The progression of the cell cycle is driven by an orchestrated interplay between genes and their protein products. During the eukaryotic cell cycle in fission yeast, the cell grows, DNA is replicated (S-phase) and divided into two daughter cells (M-phase). Between the S-phase and the M-phase there are also two gap-phases, referred to as G1 and G2. These complexities has been captured remarkably well by the pioneering work encoded in the experimentally constrained Novak and Tyson model hereby referred to as the NT-model [23], illustrated in Fig. 1. Mathematically the NT-model is defined by

$$\frac{d[\text{Cdc13}_T]}{dt} = k_1 M - (k'_2 + k''_2[\text{Ste9}] + k'''_2[\text{Slp1}])([\text{Cdc13}_T]) \quad (1)$$

$$\begin{aligned} \frac{d[\text{preMPF}]}{dt} &= k_{\text{wee}}([\text{Cdc13}_T] - [\text{preMPF}]) - k_{25}[\text{preMPF}] \\ &\quad - (k'_2 + k''_2[\text{Ste9}] + k'''_2[\text{Slp1}])([\text{preMPF}] \end{aligned} \quad (2)$$

$$\begin{aligned} \frac{d[\text{Ste9}]}{dt} &= (k'_3 + k''_3[\text{Slp1}]) \frac{1 - [\text{Ste9}]}{J_3 + 1 - [\text{Ste9}]} \\ &\quad - (k'_4[\text{SK}] + k_4[\text{MPF}]) \frac{[\text{Ste9}]}{J_4 + [\text{Ste9}]} \end{aligned} \quad (3)$$

$$\frac{d[\text{Slp1}_T]}{dt} = k'_5 + k''_5 \frac{[\text{MPF}]^4}{J_5^4 + [\text{MPF}]^4} - k_6[\text{Slp1}_T] \quad (4)$$

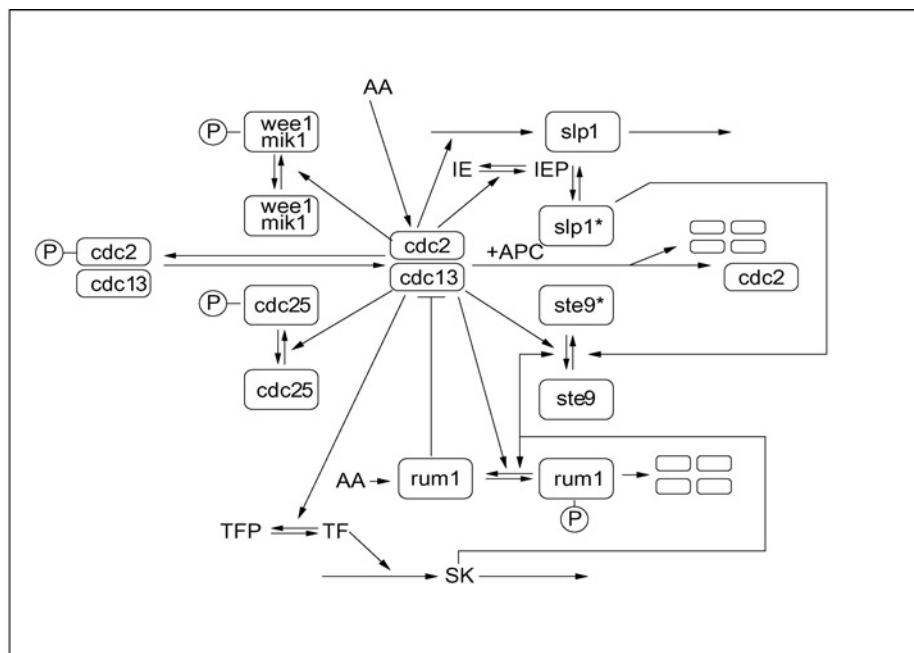
$$\begin{aligned} \frac{d[\text{Slp1}]}{dt} &= k_7[\text{IEP}] \frac{[\text{Slp1}_T] - [\text{Slp1}]}{J_7 + [\text{Slp1}_T] - [\text{Slp1}]} \\ &\quad - k_8 \frac{[\text{Slp1}]}{J_8 + [\text{Slp1}]} - k_6[\text{Slp1}] \end{aligned} \quad (5)$$

$$\frac{d[\text{IEP}]}{dt} = k_9[\text{MPF}] \frac{1 - [\text{IEP}]}{J_9 + 1 - [\text{IEP}]} - k_{10} \frac{[\text{IEP}]}{J_{10} + [\text{IEP}]} \quad (6)$$

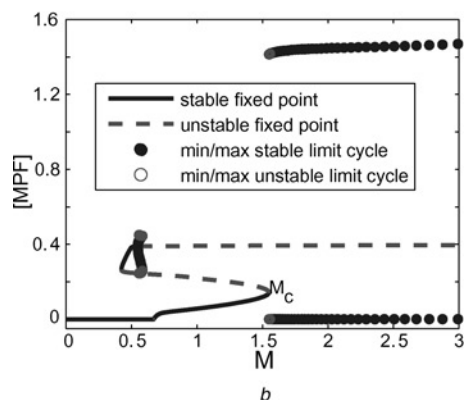
$$\frac{d[\text{Rum1}_T]}{dt} = k_{11} - (k_{12} + k'_{12}[\text{SK}] + k''_{12}[\text{MPF}])[\text{Rum1}_T] \quad (7) \quad [\text{Trimer}] = \frac{2[\text{Cdc13}_T][\text{Rum1}_T]}{\sum + \sqrt{\sum^2 - 4[\text{Cdc13}_T][\text{Rum1}_T]} \quad (10)$$

$$\frac{d[\text{SK}]}{dt} = k_{13}[\text{TF}] - k_{14}[\text{SK}] \quad (8) \quad [\text{MPF}] = \frac{([\text{Cdc13}_T] - [\text{preMPF}])([\text{Cdc13}_T] - [\text{Trimer}])}{[\text{Cdc13}_T]} \quad (11)$$

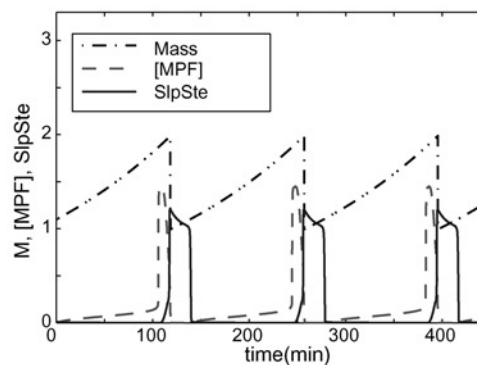
$$\frac{dM}{dt} = \mu M \quad (9) \quad [\text{TF}] = G(k_{15}M, k'_{16} + k''_{16}[\text{MPF}], J_{15}, J_{16}) \quad (12)$$



a



b



c

Figure 1 The original Novak and Tyson cell cycle model

a A wiring diagram describing the cell cycle machinery, modified from [23]

b Bifurcation diagram of the wild-type cell, (1)–(17) and parameters (18)

c Numerical simulation of the wild-type cell, (1)–(17) and parameters (18), $\text{SlpSte} = k''_2[\text{Ste9}] + k'''_2[\text{Slp1}]$. The numerical simulations were performed using XPPAUT [30] using the method QualRK (<http://www.math.pitt.edu/~bard/xpp/xpp.html>). Initial values are $[\text{Cdc13}_T] = 0.06$, $[\text{PreMPF}] = 0.04$, $[\text{Ste9}] = 0.01$, $[\text{Slp1}] = 0.0003$, $[\text{Slp1}_T] = 0.3$, $[\text{IEP}] = 0.06$, $[\text{Rum1}_T] = 0.1$, $[\text{SK}] = 0.9$ and $M = 1.1$. In b, the cell mass M is used as bifurcation parameter and $[\text{MPF}]$ is a bifurcation variable. As the mass of the cell increases above M_c , mitosis is initiated. After going through the limit cycle to the right, $[\text{MPF}]$ decreases below 0.1 and the cell mass is divided by two. The bifurcation diagram was calculated by AUTO [28] via XPPAUT and drawn by SBtoolbox [29] (www.sbtoolbox.org) for MATLAB (<http://www.mathworks.com>)

$$k_{wec} = k'_{wec} + (k''_{wec} - k'_{wec}) \frac{G(V_{awec}, V_{iwec}[\text{MPF}])}{J_{awec} J_{iwec}} \quad (13)$$

$$k_{25} = k'_{25} + (k''_{25} - k'_{25}) G(V_{a25}[\text{MPF}], V_{i25}, J_{a25}, J_{i25}) \quad (14)$$

$$\sum = [\text{Cdc13}_T] + [\text{Rum1}_T] + K_{\text{diss}} \quad (15)$$

$$G(a, b, c, d) = \frac{2ad}{b - a + bc + ad + \sqrt{(b - a + bc + ad)^2 - 4ad(b - a)}} \quad (16)$$

When [MPF] decreases below 0.1, M divides, $M \rightarrow M/2$ (17)

Parameters in the NT-model are

$$\begin{aligned} k_1 = 0.03, & \quad k'_2 = 0.03, & \quad k''_2 = 1, & \quad k'''_2 = 0.1, \\ k'_3 = 1, & \quad k''_3 = 10, & \quad J_3 = 0.01, & \quad k'_4 = 2, \\ k_4 = 35, & \quad J_4 = 0.01, & \quad k'_5 = 0.005, & \quad k''_5 = 0.3, \\ k_6 = 0.1, & \quad J_5 = 0.3, & \quad k_7 = 1, & \quad k_8 = 0.25, \\ J_7 = 0.001, & \quad J_8 = 0.001, & \quad k_9 = 0.1, & \quad k_{10} = 0.04, \\ J_9 = 0.01, & \quad J_{10} = 0.01, & \quad k_{11} = 0.1, & \quad k_{12} = 0.01, \\ k'_{12} = 1, & \quad k''_{12} = 3, & \quad K_{\text{diss}} = 0.001, & \quad k_{13} = 0.1, \\ k_{14} = 0.1, & \quad k_{15} = 1.5, & \quad k'_{16} = 1, & \quad k'_{16} = 2, \\ J_{15} = 0.01, & \quad J_{16} = 0.01, & \quad V_{awec} = 0.25, & \quad V_{iwec} = 1, \\ J_{awec} = 0.01, & \quad J_{iwec} = 0.01, & \quad V_{a25} = 1, & \quad V_{i25} = 0.25, \\ J_{a25} = 0.01, & \quad J_{i25} = 0.01, & \quad k'_{wec} = 0.15, & \quad k''_{wec} = 1.3, \\ k'_{25} = 0.05, & \quad k''_{25} = 5, & \quad \mu = 0.005. & \end{aligned} \quad (18)$$

The NT-model captures the transition between cell growth and division where the so called check-points appear as bifurcations of the system [24, 23]. The cell size is represented by the mass M of the cell, and M is a bifurcation/control parameter of the system. The system moves between different states as M increases across bifurcation points (Fig. 1b). The state of the system is monitored by the active Cdc2/Cdc13-complex, also referred to as 'M-phase promoting factor', (MPF). The MPF complex is required for the initiation of DNA replication and mitosis. A proper execution of the cell cycle requires [MPF] activity to oscillate between low (G1 phase), intermediate (S and G2 phases) and high (M phase) levels [31]. This is illustrated by a numerical simulation of the NT-model (Fig. 1c).

3 Reduction of the NT-model

Our reduction of the NT-model, first described in [25], is an iterative process based on the identification of subsets of variables behaving as switching modules, and the subsequent replacement of these by time lagged step functions. This is detailed in the Supplementary Material (S1). To identify the switching modules and determine step-function parameters,

subsets of original model variables are characterised using steady-state input/output graphs, an idea originating from [14, 25]. In order to also mimic the transient time of the subsets a time delay is used, the length of which is determined from the switching subsets, based on a step-response. The step-function parameters and the time delay is finally fine tuned from cell cycle simulations of the original model. The model reduction process results in fewer variables, since consecutive variables are lumped together and represented by a single function. The main simplification, however, is due to the reduction in rate law complexity. Instead of e.g. Michaelis–Menten or Hill-based kinetics, we use step-functions with a time delay.

By the model reduction process we implicitly make the assumptions that (i) variables have time to get sufficiently close to their steady-state before there is a significant change of input, and (ii) that the transient behaviour is not important and (iii) that the exact form of the steady-state is not critical for the system, for example, a sigmoid function can be substituted by a step-function. The idea behind the reduction is, to obtain simple enough descriptions of the dynamical modules, to enable detailed analysis. The biological relevance and justification of this procedure will be further elaborated in the discussion.

For simplicity and clear disposition, we here only consider a part of the original model, corresponding to the wild-type cell, ignoring the dynamics of variables that are mainly active when the cell size is smaller than during normal conditions. This removal of variables is based on inspection of the steady-state behaviour of the variables. Variables that have their main activity when $M < 0.8$ were replaced by constants [Supplementary Material (S1)]. This reduction has the consequence that we cannot mimic the G1/S size checkpoint of small cells. To show that a delayed piecewise linear (DPL) description is also possible when $M < 0.8$ and to mimic different mutated strains of the wild-type cell, an extended reduced model corresponding to the full NT-model is given in the Supplementary Material (S1).

3.1 The reduced model (normal cell size $M > 0.8$)

From the reduction process described in the Supplementary Material (S1) and using the notation that x represents the variables that have been approximated by step-functions, x the unmodified variables and y denotes [MPF], we obtain the following DPL system

$$\dot{x}_{\text{Cdc13}_T}(t) = -s_1(t - \tau)x_{\text{Cdc13}_T}(t) + k_1 M(t) \quad (19)$$

$$\dot{x}_{\text{PreMPF}}(t) = s_2(t)x_{\text{Cdc13}_T}(t) - s_3(t, t - \tau)x_{\text{PreMPF}}(t) \quad (20)$$

$$y_{\text{MPF}}(t) = x_{\text{Cdc13}_T}(t) - x_{\text{PreMPF}}(t) \quad (21)$$

$$s_1(t - \tau) = k'_2 + s_{\text{slp/ste}}(y_{\text{MPF}}(t - \tau)) \quad (22)$$

$$s_2(t) = s_{\text{wec}}(y_{\text{MPF}}(t)) \quad (23)$$

$$s_3(t, t - \tau) = s_{wee}(y_{MPF}(t)) + s_{25}(y_{MPF}(t)) + k'_2 + s_{slp/ste}(y_{MPF}(t - \tau)) \quad (24)$$

$$s_{25}(z) = \begin{cases} l_{25} & \text{if } z \leq \theta_{25/wee} \\ h_{25} & \text{if } z > \theta_{25/wee} \end{cases} \quad (25)$$

$$s_{wee}(z) = \begin{cases} h_{wee} & \text{if } z \leq \theta_{25/wee} \\ l_{wee} & \text{if } z > \theta_{25/wee} \end{cases} \quad (26)$$

$$s_{slp/ste}(z) = \begin{cases} l_{slp/ste} & \text{if } z \leq \theta_{slp/ste} \\ h_{slp/ste} & \text{if } z > \theta_{slp/ste} \end{cases} \quad (27)$$

Mass

$$\dot{M}(t) = \mu M(t) \quad (28)$$

when y_{MPF} decreases through 0.1, M is divided by two (29)

where the parameters are

$$\begin{aligned} \tau = 15, & \quad k_1 = 0.03, & \quad k'_2 = 0.03, & \quad l_{25} = 0.2, \\ h_{25} = 5, & \quad \theta_{25/wee} = 0.25, & \quad h_{wee} = 1.3, & \quad l_{wee} = 0.15, \\ l_{slp/ste} = 0, & \quad h_{slp/ste} = 1.3, & \quad \theta_{slp/ste} = 0.4, & \quad \mu = 0.005 \end{aligned} \quad (30)$$

The difference between this model and the model used in [25] is that we here ignore the switch of [Ste9] around [MPF] ≈ 0.9 and merge [Ste9] and [Slp1] into one module [Supplementary Material (S1)]. Consequently, the matrix A_{EM_1} of [25] disappears. There are also some minor parameter value differences.

3.1.1 Validation: To validate the performance of the reduced model as compared with the original model we performed numerical simulations. A numerical solution to the reduced models (19)–(30) is shown in Fig. 2a. Compared with a solution to the full-scale original model, (1)–(18), Fig. 1c, it is evident that the DPL system follows the dynamics of the original NT-model. To evaluate the influence of different initial conditions we compare [Supplementary Material (S3)] the outcome of 12 different sets of initial values corresponding to the NT- and DPL-model, respectively.

3.2 Mutations of the wild-type strain

In order to enable reproduction of the G1/S checkpoint of smaller cells and to mimic different mutations of the NT-model we have extended the DPL-model, so that it can also account for the region $M < 0.8$ [Supplementary Material (S1)]. Using this extended version, we defined a set of 12 mutated strains (Table 1) corresponding to those mutations of reference [32] which could easily be translated to the NT-model used in our study, as detailed in the Supplementary Table S1. The wild-type cell and

the $wee1^-$ -mutation fine-tuned the parameters. For the remaining mutations we tested how well the extended DPL-model could capture the behaviour of the original NT-model. For each mutation a numerical simulation was performed, using the extended DPL-model and the NT-model. After a transient time, three different features of the cell cycle were recorded, cell mass at birth and the length of G1-phase and the S/G2/M-phases. Eight out of twelve of these strains produce similar results when comparing the DPL- and NT-model (Table 1), the wild-type cell and the $wee1^-$ -mutation included. For three of the four mutated strains which did not resemble the NT-model, we could in retrospect identify parameter sets which give a matching behaviour between DPL- and NT-model (data not shown). The $wee1^-cdc25\Delta$ double mutation appeared to be particularly difficult to mimic by the DPL-model. This strain has the particular behaviour of ‘quantised’ cycles (inter-division times clustering around specific values [23, 32]) and as it is modelled in the NT-model, the transient behaviour of the variables are important to achieve

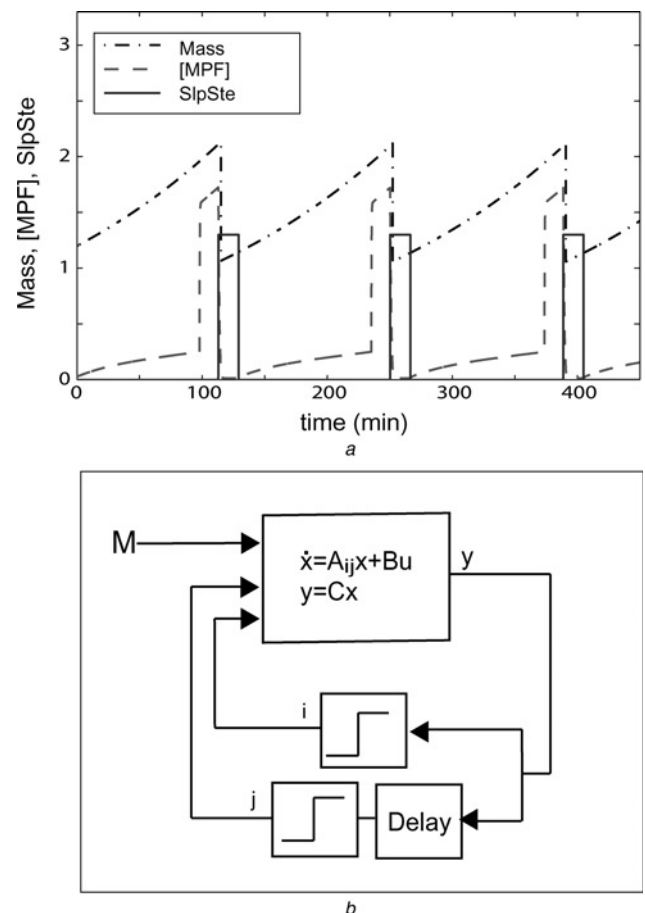


Figure 2 Illustration and validation of the DPL-model

a Validation of the DPL-model

b A control theoretical representation of the DPL-model of the wild-type cell, (19)–(29) and parameters (30). Mass = M , [MPF] = y_{MPF} and $SlpSte = s_{slp/ste}$. Initial values are $x_{cdc13t}(t_0) = 0.05$, $x_{preMPF}(t_0) = 0.02$, $M = 1.2$ and $y_{MPF}(t) < \theta_{slp/ste}$ when $t < t_0$

Table 1 Comparison between the NT- and DPL-models of simulated properties of mutant fission yeast strains

strains	Mass at birth		G1		S/G2/M		Remarks
	NT	DPL	NT	DPL	NT	DPL	
WT	0.99	1.06	28	14	111	125	~,*
<i>wee1</i> ⁻	0.50	0.45	76	78	63	61	~,*
<i>wee1</i> Δ	0.49	0.41	82	94	57	45	~,*
<i>cdc25</i> Δ	3.48	3.98	21	12	118	127	~,‡
<i>wee1</i> ⁻ <i>cdc25</i> Δ	–	1.07	–	14	–	125	≠,‡,QC
<i>wee1</i> Δ <i>cdc25</i> Δ	0.49	0.41	82	94	57	45	~,*
<i>rum1t</i> Δ	0.95	1.06	20	13	119	126	~,*
<i>rum1t</i> Δ <i>wee1</i> ⁻	0.48	0.46	73	80	66	59	~,*
<i>ste9</i> Δ	0.97	1.1	40	13	99	126	≠,‡
<i>ste9</i> Δ <i>wee1</i> ⁻	0.45	0.38	84	14	55	125	≠,‡
<i>ste9</i> Δ <i>rum1t</i> Δ	0.94	1.1	33	13	106	126	~,‡
<i>ste9</i> Δ <i>rum1t</i> Δ <i>wee1</i> ⁻	–	0.38	–	14	–	125	≠,‡,NO

~ The DPL-model captures the behaviour of the NT-model (the DPL-model mass at birth is the same as for the NT-model $\pm 20\%$, and the G1 or S/G2/M phases of the DPL-model are within ± 20 minutes of the NT-model). ≠ The DPL-model do not capture the behaviour of the NT-model. *G1 is defined as [MPF] < 0.02; ‡G1 is defined as [MPF] < 0.05. QC: The NT-model displays quantised behaviour, NO: The NT-model have no sustained oscillations

this special action. Since our reduction process is based on the steady-state behaviour and only rudimentary considers the transient parts we cannot, by definition, reproduce this mechanism.

4 Mathematical analysis of the reduced model

4.1 Matrix formulation

To facilitate analysis of stability, eigenvalues and eigenvectors the DPL model is formulated as a matrix system. Let $x = (x_{Cdc13T}, x_{PreMPF})'$ represent the state of the cell cycle system and $u_{ext} = M$ the external input, and let $y = y_{MPF}$ be the output from the cell cycle system. Then, the DPL-model can be rewritten in matrix form

$$\dot{x} = Ax + Bu_{ext}, y = Cx \quad (31)$$

where

$$C = (1 - 1), A = \begin{pmatrix} -s_1(t - \tau) & 0 \\ s_2(t) & -s_3(t, t - \tau) \end{pmatrix}$$

and s_1, s_2, s_3 are combinations of step-functions defined by (25)–(27), $B = (k_1 0)'$, and k_1 a constant parameter from the original NT-model. The system matrix A takes four possible forms, indexed by $A_{ij}, i, j \in \{1, 2\}$. A change of index i corresponds to a change of step-functions s_{25} and s_{wee} , and a change of j corresponds to a change of step-

function $s_{slp/ste}$, (26)–(30). From (22)–(24), it can be seen that j depends on $y(t - \tau)$ whereas i depends on $y(t)$, and the DPL-system therefore obeys

$$i = i(y(t)) \quad (32)$$

$$j = j(y(t - \tau)) \quad (33)$$

$$\dot{x}(t) = A_{ij}x(t) + Bu_{ext} \quad (34)$$

$$y(t) = Cx(t) \quad (35)$$

where i and j are defined by the following switching rules

$$i(y(t)) = \begin{cases} 1, & \text{if } y(t) \leq \theta_{25/wee} \\ 2, & \text{if } y(t) > \theta_{25/wee} \end{cases} \quad (36)$$

$$j(y(t - \tau)) = \begin{cases} 1, & \text{if } y(t - \tau) \leq \theta_{slp/ste} \\ 2, & \text{if } y(t - \tau) > \theta_{slp/ste} \end{cases}$$

Note that $\theta_{25/wee}$ and $\theta_{slp/ste}$ correspond to the switching thresholds of the different step-functions. The DPL-model is illustrated by the diagram in Fig. 2b. The resulting system-matrices A_{ij} correspond to

$$A_{11} = \begin{bmatrix} -(k'_2 + l_{slp/ste}) & 0 \\ h_{wee} & -(h_{wee} + l_{25} + k'_2 + l_{slp/ste}) \end{bmatrix}$$

$$A_{12} = \begin{bmatrix} -(k'_2 + h_{slp/ste}) & 0 \\ h_{wee} & -(h_{wee} + l_{25} + k'_2 + h_{slp/ste}) \end{bmatrix}$$

$$\begin{aligned}
 A_{21} &= \begin{bmatrix} -(k'_2 + l_{\text{slp}/\text{ste}}) & 0 \\ l_{\text{wee}} & -(l_{\text{wee}} + b_{25} + k'_2 + l_{\text{slp}/\text{ste}}) \end{bmatrix} \\
 A_{22} &= \begin{bmatrix} -(k'_2 + h_{\text{slp}/\text{ste}}) & 0 \\ l_{\text{wee}} & -(l_{\text{wee}} + b_{25} + k'_2 + h_{\text{slp}/\text{ste}}) \end{bmatrix}
 \end{aligned} \tag{37}$$

Here $h_{\text{slp}/\text{ste}}$, h_{wee} , b_{25} and $l_{\text{slp}/\text{ste}}$, l_{wee} , l_{25} are the high and low values of the step-functions (25)–(27) and k'_2 is a parameter from the original NT-model.

4.2 Correspondence between cell cycle phases and individual DPL-systems

To further expose the biology corresponding to the dynamical core we analysed how the four linear systems of the DPL-model correspond to the different phases within the cell cycle. The different cell cycle phases were defined based on the level of $y = [\text{MPF}]$ and on the direction of the change of $[\text{MPF}]$, i.e. whether $[\text{MPF}]$ was increasing or decreasing. We therefore have G1-phase if $[\text{MPF}] < 0.02$ and increasing, S/G2-phase if $0.02 \leq [\text{MPF}] \leq 0.25$ and increasing and M-phase if $[\text{MPF}] > 0.25$ and increasing. The phase when $[\text{MPF}]$ is decreasing was identified as completion of mitoses (denoted End M-phase). Inspection of a solution to the DPL equations gave the following relationship between cell cycle phases and linear systems (here denoted by their system matrices)

$$\begin{aligned}
 \text{G1-phase} &\sim A_{12} \\
 \text{S/G2-phase} &\sim A_{11} \\
 \text{M-phase} &\sim A_{21} \\
 \text{End M-phase} &\sim A_{22}
 \end{aligned}$$

This analysis implies that during each cell cycle phase, as defined above, one individual linear system is active. Which would mean that the protein–protein network driving the cell cycle is effectively composed of four different networks that are state-dependent.

4.3 Switching thresholds

The alternations between the individual linear systems $\dot{x}(t) = A_{ij}x(t) + Bu_{\text{ext}}$ are initiated when the output $y = [\text{MPF}]$ increases or decreases past the switching thresholds $[\text{MPF}] = \theta_{25/\text{wee}}$ or $[\text{MPF}] = \theta_{\text{slp}/\text{ste}}$ (36). The levels of these thresholds are therefore essential to the behaviour of the system. In the phase-space of x the thresholds correspond to lines and will be denoted by the immediate switching line, S^I and the delayed switching line S^D , respectively. Here S^I corresponds to the immediate change that occurs when $[\text{MPF}]$ pass $\theta_{25/\text{wee}}$, and S^D corresponds to the delayed change, which is initiated when the threshold $\theta_{\text{slp}/\text{ste}}$ is passed.

4.4 Dynamical analysis I: classification of fixed points

The DPL matrix formulation sets the stage for a dissection of fixed points and thereby elucidates the core dynamics driving the cell cycle. Using $u_{\text{ext}} = M$ as a constant parameter, each of the linear systems $\dot{x} = A_{ij}x(t) + Bu_{\text{ext}}$ has a fixed point, denoted by \hat{x}_{ij} ($= -A_{ij}^{-1}Bu_{\text{ext}}$). All A_{ij} have real negative eigenvalues and thus all fixed points are (asymptotically) stable, for all biologically relevant parameter values (e.g. $k'_2 > 0$, and all other parameters ≥ 0). Using the DPL formulation it is evident that a fixed point in a particular linear system can only be stable in the full system, if the fixed point is located in a region of the state space where this particular linear system is in use according to the switching rules.

4.4.1 Illustrative PL-example: We illustrate this insight by using a schematic PL system (Fig. 3a). For a PL system, the relationship between the fixed points and switching lines is an important dynamical property of the system. The state space of the PL system of Fig. 3a is divided into two regimes by a switching line. In the left system $S1$ drives the dynamics, whereas on the right-hand side the dynamics is governed by system $S2$. The fixed point, \hat{x}_{S1} , belongs to the same region as that in which $S1$ is defined, and all trajectories that begin in the vicinity of \hat{x}_{S1} will therefore approach this fixed point. The fixed point, \hat{x}_{S2} , is located outside the region in which $S2$ is defined. Therefore all trajectories in $S2$ are attracted by this fixed point, but they can never get close to \hat{x}_{S2} , since when they cross the border between the regions, there is a switch to system $S1$ which then governs the dynamics. We will denote the fixed point, located in the same region as that in which the corresponding linear system is used, a bona-fide fixed point (\hat{x}_{S1}), whereas a virtual fixed point refers to the case when the fixed point is positioned outside the region in which the linear system operates (\hat{x}_{S2}).

Note here that all individual linear systems of this study are by themselves asymptotically stable (all A_{ij} have real negative eigenvalues). The dynamical picture would be different, if this were not the case.

4.4.2 The DPL-model: the ‘chasing fixed point scenario’ of the cell cycle:

We will next apply our mode of analysis to the DPL-model, using the insight that the classification of the fixed points can reveal the underlying dynamics driving the cell cycle. The delay of the DPL-model makes the analysis considerably more difficult than compared with the case without delay, since at each point in the phase-space x there can be one out of two linear systems in operation, i.e. one out of two vector fields $A_{ij}x + Bu_{\text{ext}}$ determining the dynamics. We will therefore here, in the first step of our dynamical analysis, only consider fixed points in relation to the switching lines and postpone the analysis of the vector fields until Section 4.7.

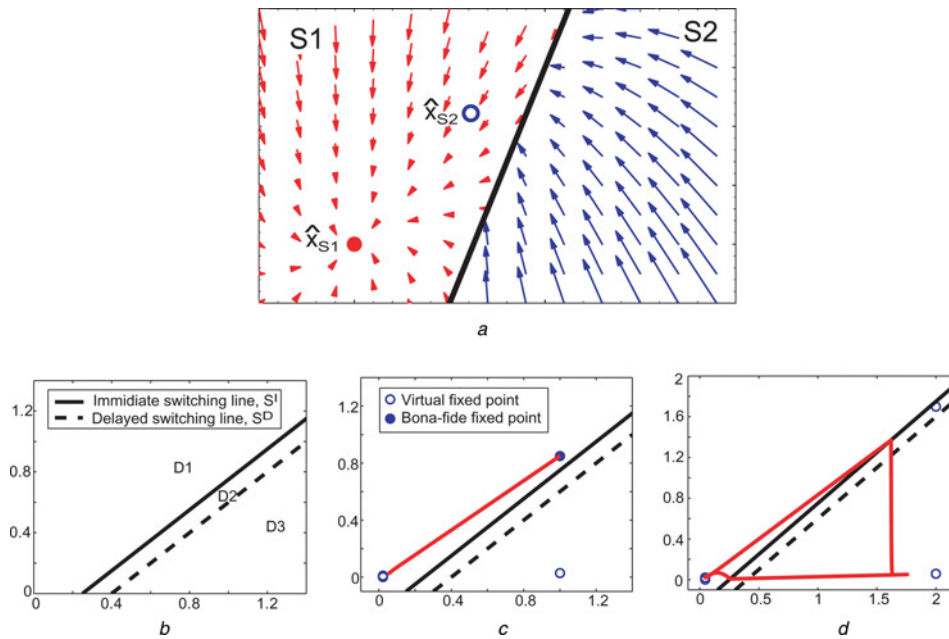


Figure 3 Classification of fixed points

- a A hypothetical example of a piecewise linear system without delay illustrating the concepts of a bona-fide fixed point (\hat{x}_{S1}), the fixed point is localised in the same domain as in which the linear system S1 is defined, and a virtual fixed point (\hat{x}_{S2}), the fixed point is situated outside the domain in which the linear system S2 is defined
- b–d Classification of fixed points of the DPL-model
- b Immediate S^I and delayed S^D switching lines of the DPL-model and subdivision of phase space into three domains $D1$, $D2$ and $D3$
- c When $M < M_c$ one fixed point is a bona-fide fixed point while the other three are virtual fixed points. A typical trajectory is approaching a stable fixed point corresponding to the bona-fide fixed point
- d When $M > M_c$ all fixed points are virtual fixed points and a typical trajectory is approaching a limit cycle. In c and d two of the virtual fixed points are almost overlapping (close to the origin)

Earlier we defined the immediate and delayed switching lines, S^I and S^D , corresponding to the switching rules (36). In the phase space of x these lines are $S^I = \{x | Cx = \theta_{25/wec}\}$ and $S^D = \{x | Cx = \theta_{slp/ste}\}$. The switching lines divide the phase space into three domains, $D1$, $D2$ and $D3$, see Fig. 3b, i.e. $D1 = \{x | 0 \leq Cx \leq \theta_{25/wec}\}$, $D2 = \{x | \theta_{25/wec} < Cx \leq \theta_{slp/ste}\}$ and $D3 = \{x | Cx > \theta_{slp/ste}\}$. The region ($Cx < 0$) consists of non-biological numerical values of x (since for biologically plausible values $[Cdc13_T] = x_{Cdc13_T} \geq [PreMPF] = x_{PreMPF}$).

We will first consider the case when $u_{ext} = M$ is treated as a constant parameter and then analyse the case when M is dynamic, $\dot{M} = \mu M$. When M is a constant parameter and $M < M_c$ (Fig. 3c) the system consists of a single bona-fide fixed point and three virtual fixed points. A trajectory of the system will typically approach the bona-fide fixed point, as time increases. This bona-fide fixed point is defined by A_{11} and thus corresponds to the S/G2-phase of the cell cycle.

When $M > M_c$, Fig. 3d, the system consists of only virtual fixed points and a trajectory will typically converge to a limit cycle. At every instant, the system moves towards a fixed point, but along its trajectory the system passes a switching line, which makes it start to chase for the next fixed point, and so forth.

When $M = M_c$, the bona-fide fixed point becomes a virtual fixed point. This corresponds to the G2/M checkpoint, i.e. the bifurcation point, M_c , of the original NT-model (Fig. 1b). When M follows $\dot{M} = \mu M$, mimicking a growing cell, then the critical threshold M_c is of importance to the final cell mass of the system (large C refers to the original system whereas small c refers to the reduced model).

One can note here that, in the DPL-model (19)–(30), which is valid when $M > 0.8$, the only cell cycle phases that correspond to a bona-fide fixed point are the S/G2-phases. This means that the G1 and M phases are here only transient and depend on the length of the time delay τ . This agrees with a recent time delay model of the cell cycle [33].

4.5 Derivation of explicit expression of cell mass

The bifurcation threshold $M = M_c$ is, as described above, of importance to the final cell mass. When M increase above this threshold, cell division is initiated. In the DPL-model, this bifurcation takes place when the fixed point $\hat{x}_{11}(M)$ ‘traverses’ the switching line S^I , i.e. when $C\hat{x}_{11}(M_c) = \theta_{25/wec}$. With this expression, we can solve for M_c explicitly in terms of model parameters. Since $\hat{x}_{11}(M_c) = -A_{11}^{-1}BM_c$, where B are defined in (31) and A_{11} in (37),

we have

$$M_C = \frac{\theta_{25/wee}(k'_2 + l_{slp/ste})(k'_2 + l_{25} + h_{wee} + l_{slp/ste})}{k_1(k'_2 + l_{25} + l_{slp/ste})} \quad (38)$$

As revealed in expression (38), there are only a few parameters that are essential for the critical value M_C . These parameters should have a large effect on final cell mass, given that the rest of the system is intact.

In the original NT-model, $M_c = 1.55$. From expression (38) and the parameter values (30) we retrieve $M_C = 1.66$. Expression (38) displays that the value M_C is sensitive for some of the chosen parameter values. For example, $\theta_{25/wee} = 0.233$ gives $M_C = 1.55$ in the DPL-model.

The final cell mass, that is, the mass before cell division, M_{end} can be calculated in the DPL-model, from the critical value M_C . In the DPL-model M_{end} corresponds to the mass at the bifurcation point M_C plus the growth of the cell during mitosis, which can be approximated with the time delay, that is

$$M_{end} = M_C e^{\mu\tau} \quad (39)$$

We compared this analytical result from the DPL-model (Fig. 4, solid line) with simulations of the original NT-model (filled circles). This was done by altering the parameter h_{wee} in (38) and perturbing the corresponding parameter k''_{wee} of the original NT-model. The DPL-model predicted the final cell mass M_{end} accurately in the

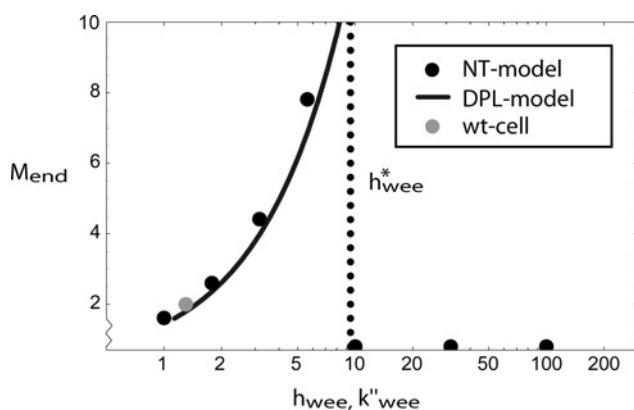


Figure 4 The DPL-model gives analytical predictions on cell cycle dynamics

Cell mass (M_{end}) as a function of h_{wee} (DPL-model) or k''_{wee} (NT-model). The solid line corresponds to the analytical result (38) and (39), from the DPLmodel (19)–(29) and parameters in (30) except for h_{wee} . When $h_{wee} = h_{wee}^*$, M_{end} is too large for constraint (41) to be satisfied and the system have collapsed (dotted black line). The filled circles correspond to M_{end} from simulations of the original NT-model after parameter perturbations to the parameter k''_{wee} . Simulations without consistent oscillations, i.e. the system has collapsed, are indicated by filled circles at the bottom of the graph

region for which it was designed ($M > 0.8$ which gives $M_{end} > 1.6$), Fig. 4.

4.6 Small background level of [Ste9] and/or [Slp1] have a large effect on cell mass – quantitative prediction from the DPL-model

The expressions (38) and (39) describe the dependence of cell mass on system parameters, and thus can give new predictions on which parameters that could influence cell mass. One such parameter is the low value of the step-function corresponding to [Ste9] and [Slp1], $l_{slp/ste}$. Using (38) and (39) we found that a small increase in $l_{slp/ste}$ would result in a large change of cell mass. As an example, to double the cell size of the wild-type cell (increase M_{end} from $M_{end} = 2$ to $M_{end} = 4$) $l_{slp/ste}$ should be increased to $l_{slp/ste} = 0.056$ (Using the parameter values in (30), except for the ‘calibrated’ value $\theta_{25/wee} = 0.233$, see the discussion about M_C above). To test this prediction from the DPL-model in the original NT-model, we made a corresponding change in the NT-model by adding a constant 0.056 to [Ste9] in (1) and (2), this gives $M_{end} = 3.9$.

4.7 Dynamical analysis II: analysis of vector fields

In order to obtain insight into the full dynamics beyond an analysis of fixed points, we examined the four vector fields $A_{ij}\mathbf{x} + B\mathbf{u}_{ext}$ of the linear systems. The crucial observation which simplified the analysis was that the dynamics most of the time was along the slow eigenvectors of the system. This set the stage for, to the best of our knowledge, the first global stability analysis of the cell cycle. This analysis showed that the cell cycle moves towards a stable fixed point when $M < M_C$ and a limit cycle when $M > M_C$, in accordance with the corresponding numerical analysis of Novak *et al.* [23]. More importantly, from this analysis we could also suggest constraints that have to be satisfied in order to keep this fixed point to limit cycle behaviour. Such constraints provide limits on possible parameter values.

4.7.1 Slow eigenvector approximation: In order to simplify a stability analysis we approximated the DPL-system with its slow eigenvectors. The rationale behind this approximation was the large difference between the eigenvalues λ_1, λ_2 of the matrices A_{ij} . This difference reflects a separation of time-scales within the system, originating from the fact that the phosphorylation of Wee1 and Cdc25 acts on PreMPF (x_{PreMPF}) but does not influence the total concentration of Cdc13 (x_{Cdc13T}). The result of the approximation was that we could consider a system trajectory as moving along, or switching between, specific lines passing through the fixed points.

Consider the homogeneous system $\dot{\mathbf{x}} = \mathbf{A}\mathbf{x}$, with initial data $\mathbf{x}(t_0) = \mathbf{x}_0$, where \mathbf{A} is a 2×2 matrix (in the interest of clarity we here only consider the homogeneous system,

since non-homogeneous systems can be transformed into this form by a translation). Assume that λ_1 and λ_2 , with $\lambda_1 \neq \lambda_2$, are the eigenvalues of A and v_1 and v_2 are the corresponding eigenvectors. Then for any initial state $x_0 = c_1 v_1 + c_2 v_2$ the solution of the linear system is $x(t) = c_1 e^{\lambda_1(t-t_0)} v_1 + c_2 e^{\lambda_2(t-t_0)} v_2$. We call the direction spanned by the eigenvector with the smallest $|\lambda|$ the slow eigendirection and the direction spanned by the eigenvector with the largest $|\lambda|$ the fast eigendirection.

With A_{ij} defined in (37) together with (30), the eigenvalues satisfy $\lambda_1, \lambda_2 < 0$ and $|\lambda_1| < |\lambda_2|$, for all A_{ij} . The largest difference between the eigenvalues is $\lambda_2 \simeq 100\lambda_1$ for A_{21} and the smallest difference is $\lambda_2 \simeq 2\lambda_1$ for A_{12} . Then $e^{\lambda_2(t-t_0)} \ll e^{\lambda_1(t-t_0)}$ as t increases. Even in the case A_{12} when the difference between the eigenvalues is smallest, for $(t - t_0) = 5$, the difference is evident $e^{\lambda_1(t-t_0)} \simeq 1 \times 10^{-3}$ and $e^{\lambda_2(t-t_0)} \simeq 7 \times 10^{-7}$. Because of this difference in eigenvalues, we approximate the dynamics of the system to the dynamics of the slow eigenvector for each of the linear systems defined by A_{ij} . We perform this approximation by assuming that $e^{\lambda_2(t-t_0)} \simeq 0$ for all $(t - t_0) > 0$. This slow eigenvector system will be referred to as the approximated DPL-system. Let us call an eigenvector that goes through the fixed point an fp-eigenvector. Then this approximation can be interpreted as, if a trajectory starts from an initial value $x(t_0)$, it will first immediately follow the fast eigenvector to either, the immediate switching line S^I , or to the slow fp-eigenvector. On the way to either of these, the delayed switching line S^D can of course also be passed, which will result in a switch between systems τ minutes later. If the trajectory reaches the immediate switching line, there is a switch to a new system. If the trajectory reaches the slow fp-eigenvector then this governs the system dynamics according to $x(t) = c_1 e^{\lambda_1(t-t_0)} v_1$, towards the fixed point. Either it stays on this fp-eigenvector as $t \rightarrow \infty$, or it switches to another system because $x(t)$ or $x(t - \tau)$ passes S^I or S^D . Fig. 5 shows a comparison between a trajectory of the ordinary DPL-

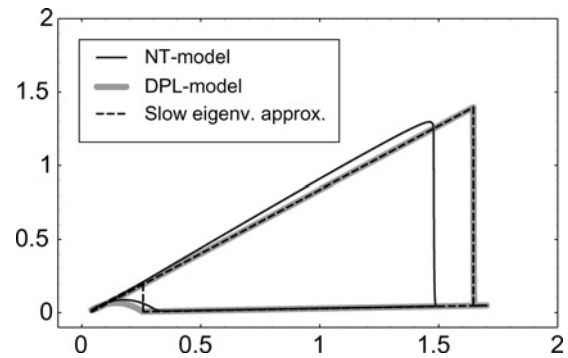


Figure 5 The DPL-model can be approximated by its slow eigenvectors

A solution to the DPL-model, the DPL-model approximated with its slow eigenvectors, and the NT-model in the phase space of x_{Cdc13t} and x_{Prempf} ([Cdc13t], [PreMPF]) using constant mass $M = 1.8$. The approximated model was solved analytically the other two numerically

system, the approximated DPL-system and the original NT-model.

4.7.2 Global stability analysis: The slow eigenvector approximation enabled us to perform a global stability analysis of the approximated DPL-model, while excluding some inappropriate initial conditions. The result of the analysis is displayed as a bifurcation diagram (Fig. 6b), which can be compared with the bifurcation analysis of the original NT-model (Fig. 6a). Below we present a theorem on global stability, but first we need to describe a restriction on possible initial conditions.

Since we have a delayed system the initial condition must not only include $x(t_0)$ but also describe the system for the last τ minutes. This is accomplished by the initial function $x(t) = f_0(t)$, $t_0 - \tau \leq t < t_0$. To exclude some numerically possible initial conditions, which are inconsistent with the

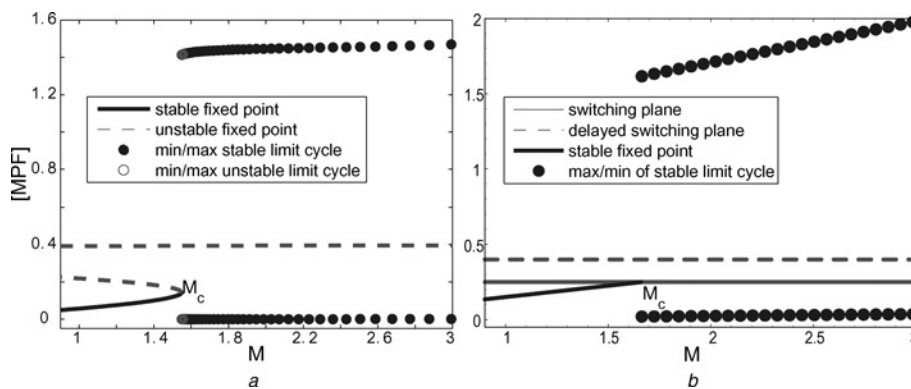


Figure 6 The approximated DPL-model captures the dynamics of the original NT-model

a Bifurcation diagram of the NT-model, (1)–(17) and parameters (18)

b Bifurcation diagram of the DPL-model, (19)–(29) and parameters (30), approximated with its slow eigenvectors. The immediate switching line corresponds to the threshold value $y_{MPF} = [MPF] = \theta_{25/wee}$ of step function $s_{25/wee}$, and the delayed switching line to $y_{MPF} = [MPF] = \theta_{slp/ste}$ of $s_{slp/ste}$. The stable fixed points for $M < M_C$ correspond to the bona-fide fixed point \hat{C}_{11}

model reduction process, we give the following restriction on 'feasible' starting conditions.

Restriction on f_0 : The initial function f_0 can only pass S^D once.

One assumption of the model reduction process, on the dynamics of the original system, was that each subsystem has sufficient time to get close to steady-state before there is a change of input. This is not satisfied for oscillations of a frequency less than τ , thus motivating this restriction. This restriction is only meaningful if it in conjunction with the DPL-model defines a closed set, i.e. a trajectory that satisfies this restriction will always satisfy this restriction under the dynamics of DPL-model. We show in Supplementary Material (S4) that this indeed is the case. We are now in a position to state and prove the following theorem.

Theorem on global stability of the cell cycle: The approximated DPL-system, under the restriction on f_0 , approaches a globally stable fixed point when $M < M_C$ and a globally stable limit cycle when $M > M_C$ as time increases.

The proof [Supplementary Material (S4)] is based on a division of all possible initial conditions that satisfy the restriction on f_0 into four groups of starting scenarios $S_1 - S_4$ (Fig. 7). We then show that a trajectory that starts

in one of these groups S_i has to either remain in that group or move to another group. This is illustrated in Fig. 7 for a constant $M > M_C$. Finally, we also show that such a trajectory approaches either a limit cycle or a fixed point.

4.7.3 Limits on parameter values retrieved from the global analysis: In Fig. 7 and the proof of global stability, Supplementary Material (S4), we showed that with the parameter set defined by (30) there exists a globally stable fixed point when $M < M_C$ and a limit cycle when $M > M_C$. From this picture we can also suggest scenarios when there will not exist a limit cycle, and therefore give constraints on model parameters, which limit the space of possible parameter values. These constraints are based on the observation that the relationships between the slow fp-eigenvectors, the fixed points and the switching lines are essential in order to have a limit cycle.

From our analysis of the DPL-model, we have found that the critical part of the cell cycle is for [MPF] to get low enough at the end of mitoses. In the original model, cell division is performed when [MPF] decreases below [MPF] = 0.1 (17). In the DPL-model this corresponds to when $y = Cx$ decreases below $Cx = 0.1$. This event is the part of the limit cycle that corresponds to starting scenario S_4 (Fig. 7c). Parameters that have a large effect on the vector field of S_4 can therefore make the system collapse.

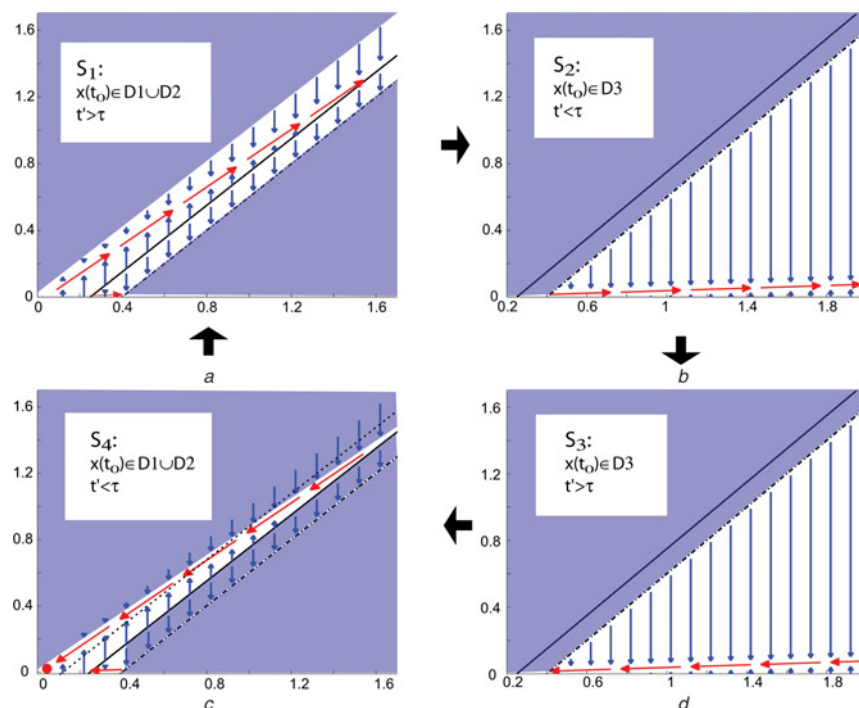


Figure 7 Illustration to the proof of the theorem of stability

a–d Vector fields of the DPL-model approximated with its slow eigenvectors, for all possible initial conditions (under the restriction on f_0) subdivided into four groups S_i , $i \in \{1, 2, 3, 4\}$. Red, slow fp-eigenvectors; blue, fast eigenvectors. A trajectory starting in any of these scenarios S_i will move to another of the scenarios. Shaded regions correspond to initial values $x(t_0)$, which are inconsistent with the S_i under concern. After a transient time all trajectories will move along slow fp-eigenvectors connected by fast eigenvectors (a limit cycle) The cell cycle follows a globally (under the restriction on f_0) stable limit cycle when $M > M_C$

For a limit cycle trajectory to decrease below $Cx = 0.1$, the slow fp-eigenvector of the linear system used in D1 of S_4 (Fig. 7c), denoted \tilde{v} , must be to the left of $Cx = 0.1$ (dotted line in Fig. 7c). In other words, $Cx < 0.1$ for some $x \in \tilde{v}$ must be satisfied. The vector \tilde{v} depends on M , $\tilde{v}(M)$. When cell division is executed $M = M_{\text{end}}$, thus, $Cx < 0.1$ for some $x \in \tilde{v}(M_{\text{end}})$. This is ensured if

$$\min_{x \in \tilde{v}(M_{\text{end}}), x \geq 0} Cx < 0.1 \quad (40)$$

Furthermore, in order to at all reach D1 of S_4 , the fixed point of the linear system used in $D2 \cup D3$ (in S_4 and S_3) must be localised in D1, leading to

$$C\hat{x}_{22}(M_{\text{end}}) < \theta_{25/wec} \quad (41)$$

In the constraints (40) and (41), M_{end} is given by (39).

Let us exemplify this finding by again analysing the role of the parameter h_{wec} which has a large effect on M_{end} . The cell cycle system works with increasing h_{wec} until M_{end} is too large and the system collapses. The first constraint which is violated when h_{wec} and M_{end} increase is (41). Let us denote the point at which this happens h_{wec}^* . The limit h_{wec}^* can be calculated by inserting (39) into (41) and solve for h_{wec} . Fig. 4 indicates when this constraint is violated and compares this prediction from the DPL-model to simulations of the original NT-model (by varying the corresponding parameter k'_{wec}).

5 Discussion

We have herein developed a procedure for how to reduce and dissect the behaviour of a nonlinear oscillatory biological control system incorporating an effective time delay. Our methodology has been developed and applied to the Novak–Tyson (NT) model of the cell cycle since the NT-model captures one of the best described and important regulatory circuits. A central notion guiding our analysis is to take advantage of biological simplifying circumstances in order to reduce the complexity of the underlying hard mathematical problem of understanding a nonlinear dynamical systems that include time delay. Below we first discuss the insights and biological simplifications that made our approach possible. We close the paper by addressing advantages and limitations with our approach by comparing with alternative strategies for understanding complex nonlinear biological control systems.

5.1 Insights from the dissection procedure which exposed the core dynamics driving the cell cycle

Our reduction of the original system and mathematical analysis enabled us to obtain insights and prove system properties beyond what is currently possible using only numerical bifurcation analysis or computer simulations.

Below we specify what can be learned from the reduction procedure, the DPL model and mathematical analysis.

5.1.1 Time-lagged steady-state approximations:

The model reduction process is based on the idea of obtaining as simple representations of the switching modules as possible. The variables are approximated by their steady-state behaviour together with a time delay. This is justified using the notion that the reduced model have the same qualitative behaviour as the original model during several conditions. By these approximations we implicitly make the assumptions that (i) variables have time to get sufficiently close to their steady-state before there is a significant change of input, and (ii) that the transient behaviour is not essential in a first approximation of understanding the core dynamics of the system and finally (iii) that the exact form of the steady-state is not critical for the system, which is to say that a sigmoid function can be replaced by a step-function. All these assumptions can of course be questioned. We have, for example, found one parameter set of the original NT-model (the *wec1⁻cdc25Δ* double mutated strain) where the transient behaviour of the modules seems to be important to achieve the particular behaviour of this strain. We have also qualitatively observed that approximating by a step-function assuming that a variable is ‘sufficiently close to their steady-state’ can actually in practice mean that the variable is only remotely at its steady-state.

In order to analyse larger complex biological networks, we believe that less detailed representations of the interacting units can be useful. Here such a coarse-grained representation is constructed by merging consecutive variables together and reducing rate-law complexity. One should note, that the original NT-model already contains several simplifying assumptions, e.g. Michaelis–Menten/Hill rate laws, and that the use of these approximation in protein signalling networks is under debate in the field [34–36]. This issue arises because the conditions required for using the pseudo steady-state approximation are rarely met, and the errors become compounded when they are used in cascades. We have, furthermore, throughout this study ignored the fact of discontinuity at the switching thresholds, which in the general case needs to be considered [37, 38].

5.1.2 Simplifying biological circumstances – modularity, switching and separation of time-scales:

Our reduction procedure of the NT-model utilises several biological circumstances such as (i) modularity, (ii) switch like response and the use of (iii) different time-scales. The reduction procedure (Section 3) relied on our identification of effective dynamical modules by careful inspection of the dependencies between the variables in the NT-model. The notion that biological circuits are organised in modules has been intensively discussed [13] and proved to be a useful tool for analysing the static organisation within large networks. However, as a rule

these studies have not included the dynamics due to lack of reliable kinetic models at this scale. Furthermore, a dynamical module defined by variable dependencies including both the strength and nature of the kinetic interactions does not necessarily coincide with a definition of modularity based on the network connectivity. Thus, for understanding system dynamics, the notion of dynamical modules appears to be a useful and biologically functionally relevant concept. Making the observation that there is a lot of switching in the NT-model we therefore defined modules exhibiting a switching dynamics, with the rationale of replacing these modules by step-functions. Considering the system when $M > 0.8$, that is, when cell mass is determined by the G2/S checkpoint, we found three modules, corresponding to the NT-variable subsets $\{k_{25}\}$, $\{k_{wee}\}$ and $\{[IEP], [Slp1t], [Slp1], [Ste9]\}$ which determined when there were abrupt changes in the system.

The second simplifying circumstance is the frequent occurrence of switching in the NT-model. This mainly due to the special form of the Michaelis–Menten-based equations used in the model, which produces steep sigmoid steady-state input–output curves, referred to as Goldbeter–Koshland functions [39]. Switching has been found in many biological systems [40–43], often modelled using a Hill-function. Biologically this phenomena can be due to cooperative processes, positive feedback or enzymes which operate near saturation [44]. The cause behind the switching and the way it is modelled (by a Hill-function, Goldbeter–Koshland dynamics etc) is not essential for our reduction process but only of relevance for interpreting the biological process generating the switch-like behaviour.

Finally, the observation that biological systems operate on different time-scales is an often used tool when reducing biological complexity. For example, the slow variable, cell mass M , has been treated by others as a constant parameter when performing bifurcation analysis of the system [23]. Similarly, we make use of the different time-scales of Cdc13 and PreMPF in the analysis of the DPL-model, by employing what is referred to as a slow eigenvector approximation. This particular separation of time-scales originates from the observation that phosphorylation of Wee1 and Cdc25 acts on PreMPF but does not influence the total concentration of Cdc13.

In summary, by removing some variables and dependencies and substituting the remaining dynamical modules with step-functions including a time delay we arrived at a minimal model formulation capturing the core dynamics driving the NT-model.

5.1.3 Validating the simplified model: To test whether our reduced model mimics the full model and implicitly assessing whether the above biological simplifications are useful we used our reduced formulation

of the NT-model to analytically derive the corresponding numerical bifurcation diagram obtained from the original NT-model. This is not possible in the full model but the very fact that we could derive the numerically computed bifurcation curve strongly validated our compact reformulation. Hence, taking this derivation and numerical simulations in the time-domain together, validated that our reduced formulation indeed generates the appropriate system dynamics. In conclusion, this result makes the suggestion that concepts and practical tools for identifying modularity, switching and separation of time-scales could be useful in reducing other complex regulatory biological circuits.

5.1.4 Understanding and exposing the core dynamics driving the cell cycle:

The reduction of the original model and exposition of the underlying simplifying biological circumstances as described above is, however, only a first step in understanding the core dynamics which represents the key underlying dynamical landscape that propels the cell cycle machinery forward in time. In particular, we are in search for a core abstract picture of what really propels a system which is not directly analysable in its raw NT-form which, however, already is a simplification of the original biological system. In Section 4.4, we therefore analysed the nature of the fixed points corresponding to the four linear systems and how the system by crossing switching planes utilises different linear subsystems. Interestingly, the biological cell cycle phases correspond to different linear subsystems in our analysis. In brief we found that a system trajectory first (when the cell mass is small) followed a (bona-fide) stable fixed point, which in itself was translocated with increasing mass. When mass increased in the limit cycle regime the trajectory started to move towards a virtual attracting fixed point, thus chasing a fixed point. With the passing of a switching line, the previous attractive virtual fixed point disappeared and the ‘next’ system matrix introduced a new virtual attractive fixed point. Such a ‘chasing fixed point’ scenario is a novel and convenient simplifying picture. This insight was not obtained from a regular numerical bifurcation analysis. Biologically this corresponds to a generalised notion of threshold (a line instead of a single threshold value) based on the dynamical modules within the system. Hence when the system passes a threshold, the state of the biological circuit is changed, leading to that a different effective subsystem of that very circuit is driving the systems dynamics. Therefore the existence of dynamical modules and the resulting fixed point/switching line analysis reveals that the protein–protein network driving the cell cycle effectively is composed of four different networks which are state-dependent, that is, depends on which switches that are passed or not. Thus a rather simple discrete on/off behaviour produces different effective systems which at the end are hidden in a complex continuous system with nonlinear time-lagged interactions. This discrete core dynamics is evidently not visible by inspection from the connectivity graph of the cell cycle.

Finally, from our analysis on the wild type cell we find that for cells of normal size ($M > 0.8$, in this study) the length of the G1 phase corresponds to the time delay of the Slp1/Ste9 module (step-function $s_{slp/ste}$). A similar result has recently been suggested in the analysis by Srividhya and Gopinathan [33] using another mathematical model of fission yeast.

Now, despite the abstract nature of the above scenario we could use the information to quantitatively predict the cell size and secondly to prove and predict conditions for the global stability of the cell cycle.

5.1.5 Prediction of cell size using the reduced core dynamical model: An important biological application of computational models is to aid us in understanding how key biological features are determined from the detailed kinetics governing the protein–protein interactions. Important biological features for the cell cycle include the average size of the cells, which depend on the size at which the individual cells divides. Ideally we would like to identify key kinetic parameters by which the cell size controls the point of cell division. Using our reduced model we could derive (Section 4.5) analytical expressions for the critical threshold M_C in terms of parameters that were derived from the original NT-model. The threshold M_C (38) reveals parameters that are important for the G2/M transition and therefore together with (39) have a large influence on final cell mass. One example is the parameter $\theta_{25/wee}$ (38). Biologically $\theta_{25/wee}$ corresponds to the threshold values of Cdc25 and Wee1 at which there is a significant increase of MPF initiating the mitoses. Furthermore, a decrease of the parameter h_{wee} should give smaller cells, a prediction which is confirmed in the original model and does not come as a surprise, since it corresponds to the biological wee^- -mutation which results in smaller cells. A more interesting result is the prediction that a small increase in the background level of [Ste9] and/or [Slp1] will have a large effect on cell size as confirmed by simulations of the original NT-model. Importantly, all these predictions are not only qualitative, but also quantitative. Hence, we do not only obtain a list of which are the crucial parameters but the formula also gives us an understanding of the dependency of the cell mass in terms of these parameters.

5.1.6 Predicting and proving asymptotic global dynamics and the stability of the cell cycle: For the best understood biological circuits, such as the cell cycle, our current understanding is as a rule captured by complex nonlinear kinetic models. The addition of biologically justified time delays clearly prohibits an analysis for the majority of circuits. From a biological perspective we would like to understand if and under what conditions the protein–protein mediated oscillations governing the cell cycle are a stable behaviour or not. In Section 4.7 we took advantage of

the observation that the circuit kinetics have different time-scales which essentially control the switching dynamics. This biological observation translates mathematically into that the system matrices have large differences in the corresponding eigenvalues. This led us to a slow eigenvector approximation which captures the essential system dynamics. This insight and additional simplification enabled a proof of the global stability of a limit cycle or fixed point solution depending on the specific value of the cell mass, illustrated by a bifurcation diagram. Since we have an explicit formula for different features of the bifurcation diagram such as critical cell mass, switching lines and fixed points, we can predict system effects of perturbations in kinetic parameters. From the global analysis of the cell cycle behaviour we can thereby identify necessary constraints on model parameters. Such constraints are helpful in order to find parameter limits, outside which the system cannot work. For example, considering the parameter h_{wee} we can calculate an upper limit of this parameter which seems to correspond to simulations of the NT-model (Fig. 4).

We are not the first to dissect the cell cycle by partitioning the system into smaller subsystems [24]. Indeed, the excellent work of Novak and Tyson displays the qualitative dynamics within different subsystems. Our study contribute a PL formulation which enables analytical analysis.

5.2 Strategies and limitations in understanding complex biological regulatory circuits

5.2.1 Simple models versus extensive computer simulations: Our work highlights the general problem on how to identify a suitable level of model complexity which is simple but yet sufficiently complex to capture the relevant dynamics underlying regulatory systems in biology. During the last century several different strategies have been developed in relation to computational modelling as a tool for describing and understanding biological systems. Biologically based computational models tend to have a large number of inhomogeneous components (different molecules and cells), governed by non-trivial interactions described by a large number of parameters that cannot as a rule be uniquely determined from experiments. Since the models are too complicated to permit direct mathematical analysis resorting to extensive computer simulations has become an important tool in understanding these systems. However, even if a large number of simulations are performed, covering only a small part of all possible parameter combinations, it is yet difficult to understand why a particular phenomena occurs in the model at hand. Therefore two successful strategies within computational neuroscience have been developed. First, a study of small systems using tools from nonlinear dynamical systems theory [45, 46]. Alternatively, formulating models which ignore a number of biological details which render these

models amenable for mean field analysis thus yielding a substantial insight into system dynamics [47]. In cases where these two approaches have not been applicable the investigator has been left to perform large-scale simulations of complicated models, an enterprise which has not proved to be as successful as initially thought. For example, in these complicated models small parameter perturbation may induce large and difficult to understand alterations in the systems dynamics. It is therefore not surprising that biologically relevant features such as time delays which make these models even more complicated have as a rule been ignored.

5.2.2 Analytical and mathematical techniques for understanding complex network models:

There are a small number of success stories when analytical techniques and reasoning have been applied for the dissection of complex models [48]. Yet, to the best of our knowledge the seminal analysis by Mackey *et al.* [49] on a small system describing white blood cells is the first where a time delay has been thoroughly analysed in a biological context. An interesting future area to explore is the relation between different levels of simplified models such as Boolean versus differential equation models [50]. Recently there has been a growing interest of developing techniques for reducing complicated computational models in systems biology [19, 51]. Ideas such as lumping and simplifying variables have been explored. This is something that will become increasingly important as more networks in different systems are characterised with increasing resolution. Tyson and Co-workers has performed pioneering work utilising nonlinear dynamical systems analysis to models of the cell cycle [24]. However, a central limitation in a mathematical approach is that the tools from numerical bifurcation analysis and mathematical analysis are limited to small systems contrasting with the larger size of biological networks. Yet, we believe that our analysis is the first to develop a systematic reduction scheme and an analysis for a time delay system which takes particular biological regularities into account to enable a reformulation of a semi-large-scale complex model to a smaller simplified model amenable for explicit mathematical analysis.

An important future problem is to investigate whether structural modularity in biological systems could facilitate reduced systems descriptions by effectively decoupling different time and spatial scales thus setting the stage for interconnected modular simplified models. Such a reduced but biologically justified system description would clearly simplify the identification of regulatory circuits from whole genome data [4].

6 Acknowledgments

We thank Dr Shohreh Maleki for helpful information regarding the biology of the cell cycle, and Camilla Trané and Doctors Erik Aurell and Albert Compte for critical

reading and discussions. This work was supported by the Lawski and Wallenberg foundations, Wennergren foundation, Stockholm University, Karolinska Institute and Linköpings University.

7 References

- [1] BARABASI A.L., OLTVAI Z.N.: 'Network biology: understanding the cell's functional organization', *Nat. Rev. Genet.*, 2004, **5**, pp. 101–113
- [2] GIALLOURAKIS C., HENSON C., REICH M., XIE X., MOOHTA V.K.: 'Disease gene discovery through integrative genomics', *Annu. Rev. Genomics Hum. Genet.*, 2005, **6**, pp. 381–406
- [3] TAN K., TEGNÉR J., RAVASI T.: 'Integrated approaches to uncovering transcription regulatory networks in mammalian cells', *Genomics*, 2008, **91**, (3), pp. 219–231
- [4] TEGNÉR J., BJÖRKEGREN J.: 'Perturbations to uncover gene networks', *Trends. Genet.*, 2007, **23**, pp. 34–41
- [5] LELOUP J.-C., GOLDBETER A.: 'A model for circadian rhythms in *Drosophila* incorporating the formation of a complex between the PER and TIM proteins', *J. Biol. Rhythms*, 1998, **13**, pp. 70–87
- [6] VON DASSOV G., MEIR E., MUNRO E.M., ODELL M.O.: 'The segment polarity network is a robust developmental module', *Nature*, 2000, **406**, pp. 188–192
- [7] ALDRIDGE B.B., BURKE J.M., LAUFFENBURGER D.A., SORGER P.K.: 'Physicochemical modelling of cell signalling pathways', *Nat. Cell. Biol.*, 2006, **8**, pp. 1195–1203
- [8] PAPIN J.A., HUNTER T., PALSSON B.O., SUBRAMANIAM S.: 'Reconstruction of cellular signalling networks and analysis of their properties', *Nat. Rev. Mol. Cell. Biol.*, 2005, **6**, pp. 99–111
- [9] GARDNER T.S., CANTOR C.R., COLLINS J.J.: 'Construction of a genetic toggle switch in *Escherichia coli*.', *Nature*, **403**, pp. 339–342
- [10] ELOWITZ M.B., LEIBLER S.: 'A synthetic oscillatory network of transcriptional regulators', *Nature*, 2000, **403**, pp. 335–338
- [11] MA'AYAN A., BLITZER R.D., IYENGAR R.: 'Toward predictive models of mammalian cells', *Annu. Rev. Biophys. Biomol. Struct.*, 2005, **34**, pp. 319–349
- [12] STOGATZ S.H.: 'Exploring complex networks', *Nature*, 2001, **410**, pp. 268–276
- [13] HARTWELL L.H., HOPFIELD J.J., LEIBLER S., MURRAY A.W.: 'From molecular to modular cell biology', *Nature*, 1999, **402**, pp. c47–c52

- [14] TYSON J.J., CHEN J.C., NOVAK B.: 'Sniffers, buffers, toggles and blinkers: dynamics of regulatory and signaling pathways in the cell', *Curr. Opin. Cell. Biol.*, 2003, **15**, pp. 221–231
- [15] ALBERT R., OTHMER H.G.: 'The topology of the regulatory interactions predicts the expression pattern of the drosophila segment polarity genes', *J. Theor. Biol.*, 2003, **223**, pp. 1–18
- [16] ELGAR A., DORFMAN R., WEISS D., ASHE H., SHILO B., BARKAI N.: 'Robustness of the BMP morphogen gradient in *Drosophila* embryonic patterning', *Nature*, 2002, **419**, pp. 304–308
- [17] ANGELI D., FERRELL JR. J.E., SONTAG E.D.: 'Detection of multistability, bifurcations, and hysteresis in a large class of biological positive-feedback systems', *Proc. Natl. Acad. Sci. USA*, 2004, **101**, pp. 1822–1827
- [18] LOVRICS A., CSIKÁSZ-NAGY A., ZSÉLY I., ZÁDOR J., TURÁNYI T., NOVÁK B.: 'Time scale and dimension analysis of a budding yeast cell cycle model', *BMC Bioinformatics*, 2006, **7**, pp. 494–505
- [19] SCHMIDT H., JACOBSEN E.W.: 'Linear systems approach to analysis of complex dynamic behaviours in biochemical networks', *IEE Syst. Biol.*, 2004, **1**, pp. 149–158
- [20] MONK N.A.M.: 'Oscillatory expression of Hes1, p53, and NF- κ B driven by transcriptional time delays', *Curr. Biol.*, 2003, **3**, pp. 1409–1413
- [21] LEWIS J.: 'Autoinhibition with transcriptional delay: a simple mechanism for the zebrafish somitogenesis oscillator', *Curr. Biol.*, 2003, **13**, pp. 1398–1408
- [22] BRATSUN D., VOLFSOON D., TSIMRING L.S., HASTY J.: 'Delay induced stochastic oscillations in gene regulation', *Proc. Natl. Acad. Sci. USA*, 2005, **102**, pp. 14593–14598
- [23] NOVAK B., PATAKI Z., CILIBERTO A., TYSON J.J.: 'Mathematical model of the cell division cycle of fission yeast', *Chaos*, 2001, **11**, pp. 277–286
- [24] TYSON J.J., CHEN A.K., NOVAK B.: 'Network dynamics and cell physiology', *Nat. Rev. Mol. Cell. Biol.*, 2001, **2**, pp. 908–916
- [25] ERIKSSON O., ZHOU Y., TEGNER J.: 'Modeling complex cellular networks – robust switching in the cell cycle ensures a piecewise linear reduction of the regulatory network'. CDC 2004: IEEE Conf. Decision and Control, 2004, vol. 1, pp. 117–123
- [26] GLASS L., KAUFFMAN S.A.: 'The logical analysis of continuous, non-linear biochemical control networks', *J. Theor. Biol.*, 1973, **39**, pp. 103–129
- [27] GLASS L.: 'Classification of biological networks by their qualitative dynamics', *J. Theor. Biol.*, 1975, **54**, pp. 85–107
- [28] DOEDEL E.J.: 'AUTO, a program for the automatic bifurcation analysis of autonomous systems', *Congr. Numer.*, 1981, **30**, pp. 265–384
- [29] SCHMIDT H., JIRSTRAND M.: 'Systems biology toolbox for MATLAB: a computational platform for research in systems biology', *Bioinformatics*, 2006, **22**, pp. 514–515
- [30] ERMENTROUT B.: 'Simulating, analyzing and animating dynamical systems: a guide to XPPAUT for researchers and students' (SIAM, Philadelphia, 2002), p. 290
- [31] TYSON J.J., CSIKÁSZ-NAGY A., NOVAK B.: 'The dynamics of cell cycle regulation', *BioEssays*, 2002, **24**, pp. 1095–1109
- [32] SVEICZER A., CSIKÁSZ-NAGY A., GYORFFY B., TYSON J., NOVAK B.: 'Modeling the fission yeast cell cycle: quantized cycle times in *wee1⁻cdc25 Δ* mutant cells', *Proc. Natl. Acad. Sci. USA*, 2000, **97**, pp. 7865–7870
- [33] SRIVIDHYA J., GOPINATHAN M.S.: 'A simple time delay model for eukaryotic cell cycle', *J. Theor. Biol.*, 2006, **241**, pp. 617–627
- [34] FARROW L.A., EDELSON D.: 'The steady-state approximation: fact or fiction?', *Int. J. Chem. Kinet.*, 1974, **6**, pp. 787–800
- [35] SEGEL L.A.: 'On the validity of the steady state assumption of enzyme kinetics', *Bull. Math. Biol.*, 1988, **50**, pp. 579–593
- [36] FLACH E.H., SCHNELL S.: 'Use and abuse of the quasi-steady-state approximation', *Syst. Biol. (Stevenage)*, 2006, **153**, pp. 187–191
- [37] DE JONG H., GOUZÉ J., HERNANDEZ C., PAGE M., SARI T., GEISELMANN J.: 'Qualitative simulation of genetic regulatory networks using piecewise-linear models', *Bull. Math. Biol.*, 2004, **66**, pp. 301–340
- [38] PLAhte E., MESTL T., OMHOLT S.W.: 'A methodological basis for description and analysis of systems with complex switch-like interactions', *J. Math. Biol.*, 1998, **36**, pp. 321–348
- [39] GOLDBETER A., KOSHLAND D.J.: 'An amplified sensitivity arising from covalent modification in biological systems', *Proc. Natl. Acad. Sci. USA*, 1981, **11**, pp. 6840–6844
- [40] HUANG C.Y., FERRELL J.E.J.: 'Ultrasensitivity in the mitogen-activated protein kinase cascade', *Proc. Natl. Acad. Sci. USA*, 1996, **93**, pp. 10078–10083
- [41] HARPER J.W.: 'A phosphorylation-driven ubiquitination switch for cell-cycle control', *Trends Cell Biol.*, 2002, **12**, pp. 104–107

- [42] HARDIE D.G., SALT I.P., HAWLEY S.A., DAVIES S.P.: 'A MP-activated protein kinase: an ultrasensitive system for monitoring cellular energy charge', *Biochem. J.*, 1999, **338**, pp. 717–722
- [43] BAGOWSKI C.P., BESSER J., FREY C.R., FERRELL J.E.J.: 'The JNK cascade as a biochemical switch in mammalian cells: ultrasensitive and all-or-none responses', *Curr. Biol.*, 2003, **13**, pp. 315–320
- [44] FERRELL J.E.J.: 'Tripping the switch fantastic: how a protein kinase cascade can convert graded inputs into switch-like outputs', *Trends Biochem. Sci.*, 1996, **21**, pp. 460–466
- [45] RINZEL J.: 'Excitation dynamics: insights from simplified membrane models', *Fed. Proc.*, 1985, **44**, pp. 2944–2946
- [46] KOPELL N.: 'Networks of neurons as dynamical systems: from geometry to biophysics', *Q. Appl. Math.*, 1998, **56**, pp. 707–718
- [47] BRUNEL N.: 'Persistent activity and the single cell f-I curve in a cortical network model', *Network*, 2000, **11**, pp. 261–280
- [48] GLASS L.: 'Synchronization and rhythmic processes in physiology', *Nature*, 2001, **410**, pp. 277–284
- [49] MACKEY M.C., GLASS L.: 'Oscillation and chaos in physiological control systems', *Science*, 1977, **197**, pp. 287–289
- [50] DAVIDICH M., BORNHOLDT S.: 'The transition from differential equations to Boolean networks: a case study in simplifying a regulatory network model', *J. Theor. Biol.*, 2008, **255**, (3), pp. 269–277
- [51] DANØ S., MADSEN M., SCHMIDT H., CEDERSUND G.: 'Reduction of a biochemical model with preservation of its basic dynamic properties', *FEBS J.*, 2006, **273**, pp. 4862–4877